Journal of Sound and Vibration (2001) **246**(3), 525–541
doi:10.1006/jsvi.2001.3672, available online at http://www.idealibrary.com on IDEAL®

CYLINDRICAL PANEL INTERIOR NOISE CONTROL USING A PAIR OF PIEZOELECTRIC ACTUATOR AND SENSOR†

O. R. Lin, Z.-X. Liu and Z.-L. Wang

Department of Engineering Mechanics Shanghai Jiao Tong University, Shanghai 200030, *People's Republic of China. E-mail: qqirong@sh*163*b.sta.net.cn*

(*Received* 21 *July* 2000, *and in final form* 1 *March* 2001)

Active control of acoustic pressure in a cylindrical cavity with a flexible cylindrical panel using a pair of piezoelectric actuator and sensor, which is one part of the cylindrical panel, is simulated. Model expansion method is used in the establishment of the state equation of the system. The active vibration control of the cylindrical panel and the interior noise reduction are performed by applying the linear quadratic Gaussian (LQG) control theory to the structural acoustic coupled system. Two cases of different external forces acting on the cylindrical panel are illustrated. The results demonstrate that such a control system can efficiently reduce the structural-borne noise.

1. INTRODUCTION

The nuclear submarine would be in danger if its sound were transmitted too far as it is easy to be detected by the enemy. So far, the reduction of sound transmission has been an important objective in many fields. One means of attempting to decrease the noise level has been through the use of passive noise control techniques such as the sound insulation and the vibration insulation, which relied on the use of stiffened and heavy materials with high damping ratio, or by redesigning the structure. This does not meet the requirements for the aircraft manufacture. Attention has turned toward active noise control technologies. In earlier active noise control techniques, an appropriate secondary sound source, which optimally interferes with the primary noise source, has been used to effect sound cancellation. The commonly used actuator for noise control applications is the traditional loudspeaker. Although this is a highly reliable sound source, it tends to become quite bulky and heavy at low frequencies where active noise control is most effective [1]. Recently, efforts have been focused on the structural-borne noise control technique by controlling vibrations of the radiating structure. The structure itself may be a noise source or the noise source can be enclosed by a structure such that the acoustic energy of the noise is transferred to the vibration energy of the structure and then reradiate. It is possible to control the radiated sound fields by suppressing those vibration modes of the structure, which are the most efficient radiators. The earliest work in the field of active structural acoustic control was published by Jones [2] and Fuller [3]. Fuller [4, 5] demonstrated through analytical and experimental investigations that the narrowband acoustic radiation

†Supported by China Shipbuilding Corporation (Contract No. 99J41.4.4).

0022-460X/01/380525 + 17 $35.00/0

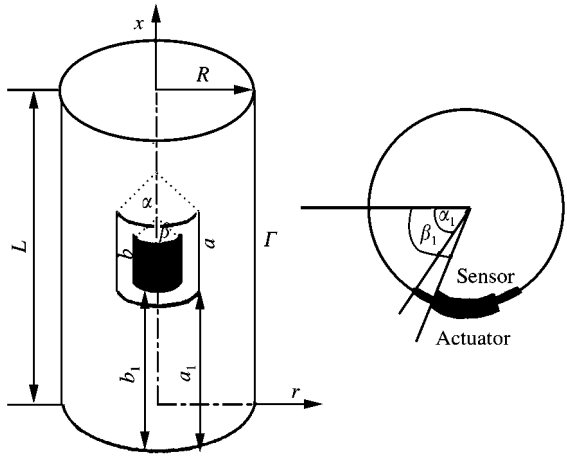

Figure 1. Configuration of a cylindrical cavity with a flexible cylindrical panel.

from the plate can be controlled by applying the active point forces to the radiating plate. This research was expanded by Clark and Fuller *et al.* [6–8] utilizing piezoceramic actuators with similar results. Sun [9] studied the shell interior noise control by neglecting the interior acoustic loading on the shell wall. The emergence of intelligent materials and structures cut a new way for the active structural acoustic control. The modelling and analysis of adaptive structural acoustic control represent a high level of sophistication and complexity. Moreover, the development of admissible mechanics for the numerical model as well as a sophisticated control algorithm for the active structural acoustic control poses a great challenge.

In this paper, the cylindrical cavity with a flexible cylindrical panel on some part of its wall is considered, as shown in Figure 1. The length and radius of the cavity is denoted by L and R. The cylindrical panel is made of aluminum, and a pair of piezoelectric actuator and sensor is perfectly attached on its inner and outer side symmetrically. The cylindrical panel covers the area $a_1 < x < a_2$, $\alpha_1 < \theta < \alpha_2$. The piezoelectric patches range over the area $b_1 < b < b_2$, $\beta_1 < \theta < \beta_2$. Meanwhile, $a = a_2 - a_1$, $\alpha = \alpha_2 - \alpha_1$, $b = b_2 - b_1$ and $\beta = \beta_2 - \beta_1$ are introduced. Since the piezoelectric actuator/sensor is very thin, its mass and stiffness to the cylindrical panel are neglected. The active vibration control and interior noise reduction can be achieved by applying optimal feedback voltage on the piezoelectric actuator so as to produce bending moment and axial tensor on the cylindrical panel. For the sake of simplicity, the cylindrical panel is assumed to be simply supported although it is not practical in applications. In our study, the structural acoustic fully coupled property is considered.

2. MODELLING OF THE STRUCTURAL ACOUSTIC FULLY COUPLED SYSTEM

For brevity, define the function $s(a_2, a_1, \alpha_2, \alpha_1)$ as $s(a_2, a_1, \alpha_2, \alpha_1) = [\mathrm{H}(x - a_2) - \mathrm{H}(x - a_1)]\,[\mathrm{H}(\theta - \alpha_2) - H(\theta - \alpha_1)]$ where $\mathrm{H}(\cdot)$ is the Heaviside function. For the acoustic field with small amplitude, its velocity potential satisfies the wave equation with uniform speed of sound c_s [10]

$$\frac{1}{r}\frac{\partial}{\partial r}\left[r\frac{\partial \phi}{\partial r}\right] - \frac{1}{c_s^2}\ddot{\phi} = -\dot{u}_r\delta(r - R)s(a_2, a_1, \alpha_2, \alpha_1), \tag{1}$$

where $\delta(\cdot)$ is the Dirac function, $\dot{(*)} = \partial(*)/\partial t$ and u_r is the deflection of the cylindrical panel in the r direction.

Flügge's equation is used to describe the motion of the cylindrical panel with a pair of piezoelectric actuator and sensor in cylindrical co-ordinates [11]:

$$L_{11}(u_x) + L_{12}(u_\theta) + L_{13}(u_r) - c\dot{u}_x - \rho h\ddot{u}_x = -q_x - f_x,$$

$$L_{21}(u_x) + L_{22}(u_\theta) + L_{23}(u_r) - c\dot{u}_\theta - \rho h\ddot{u}_\theta = -q_\theta - f_\theta,$$

$$L_{31}(u_x) + L_{32}(u_\theta) + L_{33}(u_r) - c\dot{u}_r - \rho h\ddot{u}_r = -q_r - f_r + \rho_f \dot{\phi}(r, \theta, x, t)|_{r=R}, \tag{2}$$

where the differential operator L_{ij} $(i, j = 1, 2, 3)$ are defined as

$$L_{11} = C\left[\frac{\partial^2}{\partial x^2} + (1+K)\frac{1-\mu}{2R^2}\frac{\partial^2}{\partial\theta^2}\right], \qquad L_{12} = C\frac{1+\mu}{2R}\frac{\partial^2}{\partial x\partial\theta},$$

$$L_{13} = C\left[\frac{\mu}{R}\frac{\partial}{\partial x} - KR\left(\frac{\partial^3}{\partial x^3} - \frac{1-\mu}{2R^2}\frac{\partial^3}{\partial x\delta\theta^2}\right)\right], \qquad L_{22} = C\left[(1+3K)\frac{1-\mu}{2}\frac{\partial^2}{\partial x^2} + \frac{1}{R^2}\frac{\partial^2}{\partial\theta^2}\right],$$

$$L_{23} = C\left[\frac{1}{R^2}\frac{\partial}{\partial\theta} - K\frac{3-\mu}{2}\frac{\partial^3}{\partial x^2\partial\theta}\right], \quad L_{21} = L_{12}, \quad L_{31} = -L_{13}, \quad L_{32} = -L_{23},$$

$$L_{33} = -D\left(\frac{\partial^4}{\partial x^4} + \frac{2}{R^2}\frac{\partial^4}{\partial x^2\partial\theta^2} + \frac{1}{R^4}\frac{\partial^4}{\partial\theta^4} + \frac{2}{R^4}\frac{\partial^2}{\partial\theta^2} + \frac{1}{R^4}\right) - \frac{C}{R^2}.$$

Here, $C = Eh/(1-\mu^2)$, $D = Eh^3/12(1-\mu^2)$ and $K = h^2/12R^2$. Young's modulus, the Poisson ratio, damping coefficient, thickness and density of the cylindrical panel is denoted by E, μ, c, h and ρ respectively. ρ_f is the density of the fluid and $-\rho_f\dot{\phi}(r, \theta, x, t)|_{r=R}$ is the acoustic pressure on the cylindrical panel. q_x, q_θ and q_r are the external forces in the x, θ and r direction respectively. f_x, f_θ and f_r are the equivalent forces generated by the piezoelectric actuator, and can be expressed as follows:

$$f_x = -e_{31}\frac{\partial s(b_2, b_1, \beta_2, \beta_1)}{\partial x}V(t), \qquad f_\theta = -\frac{e_{31}}{R}\frac{\partial s(b_2, b_1, \beta_2, \beta_1)}{\partial\theta}V(t),$$

$$f_r = -e_{31}\left[\frac{h+h_p}{2}\left(\frac{\partial^2 s(b_2, b_1, \beta_2, \beta_1)}{\partial x^2} + \frac{1}{R^2}\frac{\partial^2 s(b_2, b_1, \beta_2, \beta_1)}{\partial\theta^2}\right) - \frac{s(b_2, b_1, \beta_2, \beta_1)}{R}\right]V(t), \tag{3}$$

where e_{31} and h_p are the piezoelectric constant and thickness of the piezoelectric patch respectively. The boundaries of the cylindrical cavity denoted by Γ are taken to be hard walls thus leading to the zero normal velocity boundary conditions:

$$\nabla\Phi\cdot\hat{n} = 0 \quad (r, x, \theta) \in \Gamma. \tag{4}$$

The boundary conditions of the simply supported cylindrical panel are

$$M_{\theta\theta}|_{x=a_1, a_2} = 0, \quad M_{xx}|_{\theta=\alpha_1, \alpha_2} = 0,$$

$$u_x = u_\theta = u_r = 0 \quad \text{on } x = a_1 \quad \text{or} \quad x = a_2 \quad \text{or} \quad \theta = \alpha_1 \quad \text{or} \quad \theta = \alpha_2, \tag{5}$$

where

$$M_{\theta\theta} = D(K_{\theta\theta} + \mu K_{xx}), \quad M_{xx} = D(K_{xx} + \mu K_{\theta\theta}), \text{ and } K_{\theta\theta} = \frac{1}{R^2}\left(\frac{\partial u_\theta}{\partial \theta} - \frac{\partial^2 u_r}{\partial \theta^2}\right),$$

$$K_{xx} = -\frac{\partial^2 u_r}{\partial x^2}.$$

The initial conditions of the structural acoustic system are

$$\phi(r, x, \theta, t)|_{t=0} = 0, \qquad \dot{\phi}(r, x, \theta, t)|_{t=0} = 0, \tag{6}$$

$$u_x(x, \theta, t)|_{t=0} = 0, \qquad \dot{u}_x(x, \theta, t)|_{t=0} = 0,$$

$$u_\theta(x, \theta, t)|_{t=0} = 0, \qquad \dot{u}_\theta(x, \theta, t)|_{t=0} = 0,$$

$$u_r(x, \theta, t)|_{t=0} = 0, \qquad \dot{u}_r(x, \theta, t)|_{t=0} = 0. \tag{7}$$

3. MODAL ANALYSIS OF A CYLINDRICAL PANEL

For a simply supported cylindrical panel, the fire vibration at a natural frequency ω can be assumed in the following form:

$$u_x = U_x(x, \theta)\, e^{i\omega t}, \qquad u_\theta = U_\theta(x, \theta) e^{i\omega t}, \qquad u_r = U_r(x, \theta) e^{i\omega t}, \tag{8}$$

where

$$U_x(x, \theta) = A_{mn} \cos\frac{m\pi(x - a_1)}{a} \sin\frac{n\pi(\theta - \alpha_1)}{\alpha},$$

$$U_\theta(x, \theta) = B_{mn} \sin\frac{m\pi(x - a_1)}{a} \cos\frac{n\pi(\theta - \alpha_1)}{\alpha},$$

$$U_r(x, \theta) = C_{mn} \sin\frac{m\pi(x - a_1)}{a} \sin\frac{n\pi(\theta - \alpha_1)}{\alpha}. \tag{9}$$

Then substitution of equation (8) into equation (2) whose right-hand side is set to zero yields:

$$\begin{bmatrix} \rho h\omega^2 - k_{11} & k_{12} & k_{13} \\ k_{12} & \rho h\omega^2 - k_{22} & k_{23} \\ k_{13} & k_{23} & \rho h\omega^2 - k_{33} \end{bmatrix} \begin{Bmatrix} A_{nm} \\ B_{nm} \\ C_{mn} \end{Bmatrix} = \{0\}, \tag{10}$$

where the constants k_{ij} $(i, j = 1, 2, 3)$ are given as

$$k_{11} = C\left[\left(\frac{m\pi}{a}\right)^2 + (1 + K)\frac{1 - \mu}{2R^2}\left(\frac{n\pi}{\alpha}\right)^2\right], \qquad k_{12} = -C\frac{1 + \mu}{2R}\frac{m\pi}{a}\frac{n\pi}{\alpha},$$

$$k_{13} = C\left[\frac{\mu}{R}\frac{m\pi}{a} + KR\left(\left(\frac{m\pi}{a}\right)^3 - \frac{1 - \mu}{2R^2}\frac{m\pi}{a}\left(\frac{n\pi}{\alpha}\right)^2\right)\right],$$

$$k_{22} = C\left[(1+3K)\frac{1-\mu}{2}\left(\frac{m\pi}{a}\right)^2 + \frac{1}{R^2}\left(\frac{n\pi}{\alpha}\right)^2\right], \qquad k_{23} = C\left[K\frac{3-\mu}{2}\left(\frac{m\pi}{a}\right)^2\frac{n\pi}{\alpha} + \frac{1}{R^2}\left(\frac{n\pi}{\alpha}\right)^2\right],$$

$$k_{33} = D\left(\left(\frac{m\pi}{a}\right)^4 + \frac{2}{R^2}\left(\frac{m\pi}{a}\right)^2\left(\frac{n\pi}{\alpha}\right)^2 + \frac{1}{R^4}\left(\frac{n\pi}{\alpha}\right)^4 - \frac{2}{R^4}\left(\frac{n\pi}{\alpha}\right)^2 + \frac{1}{R^4}\right) + \frac{C}{R^2}.$$

Setting the determinant of this matrix to zero for a non-trivial solution yields the characteristic equation $\omega^6 + \lambda_1\omega^4 + \lambda_2\omega^2 + \lambda_3 = 0$, where the constants $\lambda_i\,(i = 1, 2, 3)$ are given as

$$\lambda_1 = -\frac{1}{\rho h}(k_{11} + k_{22} + k_{33}),\ \lambda_2 = \frac{1}{(\rho h)^2}(k_{11}k_{33} + k_{22}k_{33} + k_{11}k_{22} - k_{12}^2 - k_{23}^2 - k_{13}^2),$$

$$\lambda_3 = \frac{1}{(\rho h)^3}(k_{11}k_{23}^2 + k_{22}k_{13}^2 + k_{33}k_{12}^2 + 2k_{12}k_{13}k_{23} - k_{11}k_{22}k_{33}).$$

The roots of the above equation can be written as

$$\omega_1^2 = -\frac{2}{3}\sqrt{a_1^2 - 3a_2}\cos\frac{\psi}{3} - \frac{a_1}{3}, \qquad \omega_2^2 = -\frac{2}{3}\sqrt{a_1^2 - 3a_2}\cos\frac{\psi + 2\pi}{3} - \frac{a_1}{3},$$

$$\omega_3^2 = -\frac{2}{3}\sqrt{a_1^2 - 3a_2}\cos\frac{\psi + 4\pi}{3} - \frac{a_1}{3}, \tag{11}$$

where $\psi = ar\cos(2a_1^3 - 9a_1a_2 + 27a_3)/2\sqrt{(a_1^2 - 3a_2)^3}$.

Thus, the modes of the cylindrical panel can be obtained as

$$\frac{A_{imn}}{C_{imn}} = -\frac{k_{13}(\rho h\omega_i^2 - k_{22}) - k_{12}k_{23}}{(\rho h\omega_i^2 - k_{11})(\rho h\omega_i^2 - k_{22}) - k_{12}^2},$$

$$\frac{B_{imn}}{C_{imn}} = -\frac{k_{23}(\rho h\omega_i^2 - k_{11}) - k_{12}k_{13}}{(\rho h\omega_i^2 - k_{11})(\rho h\omega_i^2 - k_{22}) - k_{12}^2} \quad (i = 1, 2, 3). \tag{12}$$

4. MODAL ANALYSIS OF THE INTERIOR ACOUSTIC FIELD

At a natural frequency $\bar{\omega}$, the free vibration of the acoustic field in the cylindrical cavity can be assumed as

$$\phi(r, x, \theta, t) = \Phi(r, x, \theta)\,e^{i\bar{\omega}t}, \quad \Phi(r, x, \theta) = f(r)\cos\frac{p\pi x}{L}\cos q\theta. \tag{13}$$

Substitution of the above equation into equation (1) yields the characteristic equation

$$\frac{1}{r}\frac{d}{dr}\left[r\frac{df(r)}{dr}\right] + \left[\chi_p^2 - \frac{q^2}{r^2}\right]f(r) = 0 \quad \text{and} \quad f(0) \text{ is limited}, \tag{14}$$

where $\chi_p^2 = (\bar{\omega}/c_s)^2 - (p\pi/L)^2$.

The solution of equation (14) can be expressed in the q order Bessel function of the first kind when χ_p is real as $f(r) = H \cdot J_q(\chi_p r)$, in this case $\bar{\omega}^2 = (\chi_p^2 + (p\pi/L)^2)\,c_s^2$; when χ_p is

imaginary, set $\chi_p = \bar{\chi}_p \mathrm{i}$, thus the solution of equation (14) can be written in the q order modified Bessel function of the first kind as $f(r) = H \cdot \mathrm{I}_q(\bar{\chi}_p r)$, then $\bar{\omega}^2 = ((p\pi/L)^2 - \bar{\chi}_p^2)\, c_s^2$. Here, H is an arbitrary constant. The constant χ_p or $\bar{\chi}_p$ is determined by the boundary condition $\mathrm{d}f(r)/\mathrm{d}r = 0$, that is,

$$-\chi_p \mathrm{J}_{q+1}(\chi_p R) + \frac{q}{R}\mathrm{J}_q(\chi_p R) = 0, \quad \text{or} \quad \bar{\chi}_p \mathrm{I}_{q+1}(\bar{\chi}_p R) + \frac{q}{R}\mathrm{I}_q(\bar{\chi}_p R) = 0. \tag{15}$$

In addition, the orthogonal characteristics of the Bessel function of the first kind can be expressed as

$$\int_0^R \mathrm{J}_q(\chi_{pi} r)\,\mathrm{J}_q(\chi_{pj} r)\, r\, \mathrm{d}r = \begin{cases} 0, & \chi_{pj} \neq \chi_{pi}, \\ \dfrac{1}{2}\mathrm{J}_q^2(\chi_{pi} R)\left(R^2 - \dfrac{q^2}{\chi_{pi}^2}\right), & \chi_{pj} = \chi_{pi} \end{cases} \tag{16}$$

and the orthogonal relationship of the modified Bessel function of the first kind is

$$\int_0^R \mathrm{I}_q(\bar{\chi}_{pi} r)\,\mathrm{I}_q(\bar{\chi}_{pj} r)\, r\, \mathrm{d}r = \begin{cases} 0, & \bar{\chi}_{pj} \neq \bar{\chi}_{pi}, \\ \dfrac{1}{2}\mathrm{I}_q^2(\bar{\chi}_{pi} R)\left(R^2 + \dfrac{q^2}{\bar{\chi}_{pi}^2}\right), & \bar{\chi}_{pj} = \bar{\chi}_{pi}. \end{cases} \tag{17}$$

5. ANALYSIS OF THE STRUCTURAL ACOUSTIC FULLY COUPLED SYSTEM

By using the modal expansion method, the forced vibration of the acoustic field is assumed as

$$\phi(r, x, \theta, t) = \sum_{g=1}^{g_\Phi} \sum_{p=1}^{p_\Phi} \sum_{q=1}^{q_\Phi} \Phi_{gpq}(r, x, \theta)\, \zeta_{gpq}(t), \tag{18}$$

where $\Phi_{gpq}(r, x, \theta) = H_{gpq}\mathrm{J}_q(\chi_{pg} r)\cos(p\pi x/L)\cos q\theta$.

The forced vibration of the cylindrical panel are expressed in the following form:

$$u_x = \sum_{m=1}^{m_{cp}} \sum_{n=1}^{n_{cp}} U_{xmn}(x, \theta)\,\eta_{mn}(t), \quad u_\theta = \sum_{m=1}^{m_{cp}} \sum_{n=1}^{n_{cp}} U_{\theta mn}(x, \theta)\,\eta_{mn}(t), \quad u_r = \sum_{m=1}^{m_{cp}} \sum_{n=1}^{n_{cp}} U_{rmn}(x, \theta)\,\eta_{mn}(t). \tag{19}$$

Insertion of equations (18) and (19) into equation (1) yields

$$\ddot{\zeta}_{gpq}(t) + \bar{\omega}_{gpq}^2\, \zeta_{gpq}(t) = \sum_{m=1}^{m_{cp}} \sum_{n=1}^{n_{cp}} F_{qpqmn}\, \dot{\eta}_{mn}(t), \tag{20}$$

where

$$F_{gpqmn} = \frac{4c_s^2\, RC_{mn}\gamma_1\gamma_2}{H_{gpq}\mathrm{J}_q(\chi_{pg} R)\,(R^2 - q^2/\chi_{pg}^2)\pi L}, \quad \gamma_1 = \int_{a_1}^{a_1 + a} \sin\frac{m\pi(x - a_1)}{a}\cos\frac{p\pi x}{L}\,\mathrm{d}x,$$

$$\gamma_2 = \int_{\alpha_1}^{\alpha_1 + \alpha} \sin\frac{m\pi(\theta - \alpha_1)}{\alpha}\cos q\theta\,\mathrm{d}\theta.$$

Insertion of equations (18) and (19) into equation (2) yields

$$\ddot{\eta}_{mn}(t) + \frac{c}{\rho h}\dot{\eta}_{mn}(t) + \omega_{mn}^2\eta_{mn}(t) = q_{mn} + M_{Vmn}V(t) + \sum_{g}^{g_\Phi}\sum_{p}^{p_\Phi}\sum_{q}^{q_\Phi} M_{\Phi mngpq}\dot{\xi}_{gpq}(t), \tag{21}$$

where $q_{mn} = (1/\rho h\sum_{mn})\int_{a_1}^{a_2}\int_{\alpha_1}^{\alpha_2}(q_x U_{xmn} + q_\theta U_{\theta mn} + q_r U_{rmn})\,\mathrm{d}x\,\mathrm{d}\theta$,

$$M_{Vmn} = \frac{e_{31}}{\rho h\sum_{mn}}\left[A_{mn}\frac{\alpha}{n\pi} + B_{mn}\frac{1}{R}\frac{a}{m\pi} + C_{mn}\left(\frac{1}{R}\frac{a}{m\pi}\frac{\alpha}{n\pi} - \frac{h+h_p}{2}\left(\frac{1}{R^2}\frac{a}{m}\frac{n}{\alpha} + \frac{m}{a}\frac{\alpha}{n}\right)\right)\right]$$

$$\left(\cos\frac{m\pi(b_2-a_1)}{a} - \cos\frac{m\pi(b_1-a_1)}{a}\right)\left(\cos\frac{n\pi(\beta_2-\alpha_1)}{\alpha} - \cos\frac{n\pi(\beta_1-\alpha_1)}{\alpha}\right),$$

$$M_{\Phi mngpq} = \frac{-1}{\rho h\sum_{mn}}\,\rho_f H_{gpq}\mathrm{J}_q(\chi_{pg}R)C_{mn}\gamma_1\gamma_2,$$

$$\sum_{mn} = \int_{a_1}^{a_2}\int_{\alpha_1}^{\alpha_2}\rho h(U_{xmn}^2 + U_{\theta mn}^2 + U_{rmn}^2)\,\mathrm{d}x\,\mathrm{d}\theta = (A_{mn}^2 + B_{mn}^2 + C_{mn}^2)\frac{a\alpha}{4}. \tag{22}$$

The closed-circuit output charge of the piezoelectric sensor can be written as

$$Q_e = e_{31}R\iint_{s^p}(\varepsilon_{xx} + \varepsilon_{\theta\theta})\,\mathrm{d}x\,\mathrm{d}\theta, \tag{23}$$

where

$$\varepsilon_{xx} = \frac{\partial u_x}{\partial x} + \frac{h}{2}\frac{\partial^2 u_r}{\partial x^2}, \quad \varepsilon_{\theta\theta} = \frac{1}{R}(\partial u_\theta/\partial\theta + u_r) - (h/2R^2)(\partial u_\theta/\partial\theta - \partial^2 u_r/\partial\theta^2).$$

Thus, the output electric current of the sensor can be obtained as

$$i_e = \frac{\mathrm{d}Q_e}{\mathrm{d}t} = \sum_{m=1}^{m_{cp}}\sum_{n=1}^{n_{cp}} M_{Qmn}\dot{\eta}_{mn}(t), \tag{24}$$

where

$$M_{Qmn} = e_{31}R\left[-A_{mn}\frac{m\pi}{a} - B_{mn}\frac{n\pi}{\alpha}\left(\frac{1}{R} - \frac{h}{2R^2}\right) - C_{mn}\left(\frac{1}{R} - \frac{h}{2R^2}\left(\frac{n\pi}{\alpha}\right)^2 - \frac{h}{2}\left(\frac{m\pi}{a}\right)^2\right)\right]$$

$$\left(\cos\frac{m\pi(b_2-a_1)}{a} - \cos\frac{m\pi(b_1-a_1)}{a}\right)\left(\cos\frac{n\pi(\beta_2-\alpha_1)}{\alpha} - \cos\frac{n\pi(\beta_1-\alpha_1)}{\alpha}\right)\frac{m\pi}{a}\frac{n\pi}{\alpha}.$$

Then the model of the acoustic field can be cast in the state-space from as follows:

$$\dot{x}_\Phi = A_\Phi x_\Phi + B_\Phi u_\Phi, \qquad y_\Phi = C_\Phi x_\Phi + D_\Phi u_\Phi, \tag{25}$$

where

$$x_\Phi = \begin{Bmatrix}\{\zeta\}\\ \{\dot{\zeta}\}\end{Bmatrix}, \quad u_\Phi = \{\dot{\eta}_{mn}\}, \; A_\Phi = \begin{bmatrix}0 & I\\ -\Omega_\Phi^2 & -2\xi_\Phi\Omega_\Phi\end{bmatrix}, \quad B_\Phi = \begin{bmatrix}0\\ F_{gpqmn}\end{bmatrix}, \; C_\Phi = [0,\; I],$$

$D_\Phi = [0]$, $\Omega_\Phi = \mathrm{diag}(\bar{\omega}_{gpq})$, ξ_Φ is the damping ratio of the acoustic field.

Also, the model of the cylindrical panel is cast in the state-space form as follows:

$$\dot{x}_{cp} = A_{cp}x_{cp} + B_{cp}u_{cp}, \qquad y_{cp} = C_{cp}x_{cp} + D_{cp}u_{cp}, \tag{26}$$

where

$$x_{cp} = \begin{Bmatrix} \{\eta\} \\ \{\dot{\eta}\} \end{Bmatrix}, \quad u_{cp} = \{Q_f\} + [M_\Phi]\{\ddot{\zeta}_{gpq}\} + \{M_V\}V(t), \; \{Q_f\} = \{q_{mn}\}, \; [M_\Phi] = [M_{\Phi mngpq}],$$

$$\{M_V\} = \{M_{Vmn}\}, \quad A_{cp} = \begin{bmatrix} 0 & I \\ -\Omega_{cp}^2 & -C_{Dcp} \end{bmatrix}, \quad B_{cp} = \begin{bmatrix} 0 \\ I \end{bmatrix}, \quad C_{cp} = [0 \;\; M_Q], \; D_{cp} = [0],$$

$$\Omega_{cp} = \text{diag}(\omega_{mn}), \; C_{Dcp} = \text{diag}\left(\frac{c}{\rho h}\right), \; M_Q = [M_{Qmn}].$$

6. CONTROLLER DESIGN

A linear quadratic optimal controller is designed to suppress the vibration of the cylindrical panel and the acoustic pressure in the cavity, and it requires that all the states should be available. In practice, only a few states can be measured. So, one should design an observer to estimate the states from the measured signal. Among several proposed observers, the Kalman filter is selected in this study, and it is an optimal state estimator for a system contaminated with process and measurement noise [12]. The state-space equation for a system with external noise can be written as follows:

$$\dot{x}_{cp} = A_{cp}x_{cp} + B_{cp}u_{cp} + Gw, \qquad y_{cp} = C_{cp}x_{cp} + D_{cp}u_{cp} + v. \tag{27}$$

Here, assume that $G = B_{cp}$, process noise w and measurement noise v are both white noise. Moreover, they are not correlated to each other. That is,

$$E\{w\} = 0, \quad E\{v\} = 0, \quad E\{ww^{\mathrm{T}}\} = \hat{Q}, \quad E\{vv^{\mathrm{T}}\} = \hat{R}, \quad E\{wv^{\mathrm{T}}\} = 0, \tag{28}$$

where $\hat{Q}$ is a semi-positive-defined matrix and $\hat{R}$ is the positively defined matrix.

The Kalman filter dynamics can be written as

$$\dot{\hat{x}}_{cp} = A_{cp}\hat{x}_{cp} + B_{cp}u_{cp} + \hat{L}(y - C_{cp}\hat{x} - D_{cp}u_{cp}), \tag{29}$$

where $\hat{x}_{cp}$ is an estimated state and $\hat{L}$ is the Kalman filter gain to minimize the expected value $J = E\{(x_{cp} - \hat{x}_{cp})^{\mathrm{T}}(x_{cp} - \hat{x}_{cp})\}$. The filter gain $\hat{L}$ can be obtained form equation (30) and the algebraic Riccati equation (31):

$$\hat{L} = \hat{P}C_{cp}^{\mathrm{T}}\hat{R}^{-1}, \tag{30}$$

$$A_{cp}\hat{P} + \hat{P}A_{cp}^{\mathrm{T}} - \hat{P}C_{cp}^{\mathrm{T}}\hat{R}^{-1}C_{cp}\hat{P} + G\hat{Q}G^{\mathrm{T}} = 0. \tag{31}$$

Active vibration control and noise reduction is achieved by applying the optimal voltage V on the piezoelectric actuator. In order to design the optimal controller, the state equation of the cylindrical panel excited only by the actuator equivalent forces is written as

$$\dot{x}_{cp} = \bar{A}_{cp}x_{cp} + \bar{B}_{cp}V, \qquad \bar{y}_{cp} = \bar{C}_{cp}x_{cp} + \bar{D}_{cp}V, \tag{32}$$

where

$$\bar{A}_{cp} = A_{cp}, \; \bar{B}_{cp} = \begin{Bmatrix} 0 \\ M_V \end{Bmatrix}, \; \bar{C}_{cp} = C_{cp}, \quad \bar{D}_{cp} = \{0\}.$$

The objective function J for the vibration and noise reduction is chosen as $J = \lim_{T\to\infty}(1/2T)\int_{-T}^{T}(x_{cp}^{\mathrm{T}}\bar{Q}x_{cp} + V^{\mathrm{T}}\bar{R}V)\,\mathrm{d}t$ where $\bar{Q}$ is the performance weighting and $\bar{R}$ is the control

effort penalty. Moreover, the control voltage must meet $|\max(V(t))| \leqslant V_{max}$. Thus, the optimal control voltage can be written as

$$V = -K\hat{x}_{cp}, \tag{33}$$

where K is the optimal gain. It can be obtained from equation (34) and the algebraic Riccati equation (35):

$$K = \bar{R}^{-1}\bar{B}_{cp}^{\mathrm{T}}\bar{P}, \tag{34}$$

$$\bar{A}_{cp}^{\mathrm{T}}\bar{P} + \bar{P}\bar{A}_{cp} - \bar{P}\bar{B}_{cp}\bar{R}^{-1}\bar{B}_{cp}^{\mathrm{T}}\bar{P} + \bar{Q} = 0. \tag{35}$$

As discussed so far, a control procedure which uses a Kalman filter as an estimator and a controller that minimizes an objective function of quadratic form is called an LQG control method. In order to maintain the system as controllable and observable, the location of the piezoelectric actuator and sensor must be optimized so that both M_V and M_Q are not zero.

7. NUMERICAL SIMULATION

The configuration of the structural acoustic coupled system is shown in Figure 1. Its geometrical and mechanical properties are given in Table 1.

Two cases of different forces acting on the cylindrical panel such as impulse and resonant distributed force are illustrated in the following demonstration. From numerical tests, it was found that the simulation can be fully resolved with the choise $g_\Phi = 10$, $p_\Phi = 10$, $q_\Phi = 10$, $m_{cp} = 8$, $n_{cp} = 8$ and the following results were obtained with these values. It should be noted that the acoustic pressure in these figures is at the point $(r, \theta, x) = (R/2, L/2, 0)$ and the measured and estimated displacements in these figures are at the center of the cylindrical panel.

TABLE 1

Geometrical and mechanical properties

L (m)	1·5
R (m)	0·3
a_1 (m)	0·5
a_2 (m)	0·85
α_1 (rad)	0
α_2 (rad)	$\pi/3$
h (m)	0·001
b_1 (m)	0·53
b_2 (m)	0·79
β_1 (rad)	$\pi/15$
h_p (m)	0·0003
β_2 (rad)	$\pi/4$
E (Pa)	$7{\cdot}1 \times 10^{10}$
μ	0·3
ρ (kg/m^3)	2700
c (kg m/s)	100
ρ_f (kg/m^3)	1·21
ξ_Φ	0·05
c_s (m/s)	343
e_{31} (c/m^2)	− 5·2

TABLE 2

Natural frequencies of the cylindrical panel (Hz)

n	$m=1$	$m=2$	$m=3$	$m=4$	$m=5$	$m=6$	$m=7$	$m=8$
1	1162·3	2052·7	2389·9	2543·7	2641·6	2730·8	2834·3	2966·8
2	463·4	1212·8	1764·1	2110·8	2342·4	2523·0	2691·4	2871·8
3	325·3	772·0	1271·3	1684·3	2008·3	2274·6	2515·1	2754·6
4	430·8	653·7	1019·2	1402·7	1754·4	2071·5	2367·9	2660·4
5	638·7	758·6	999·5	1311·3	1643·3	1973·7	2300·2	2629·1
6	906·7	989·7	1156·8	1399·6	1690·8	2007·9	2340·6	2687·1
7	1226·7	1296·3	1428·2	1625·4	1877·7	2171·1	2494·9	2844·0
8	1596·7	1661·0	1776·8	1948·3	2172·9	2443·7	2753·5	3096·8

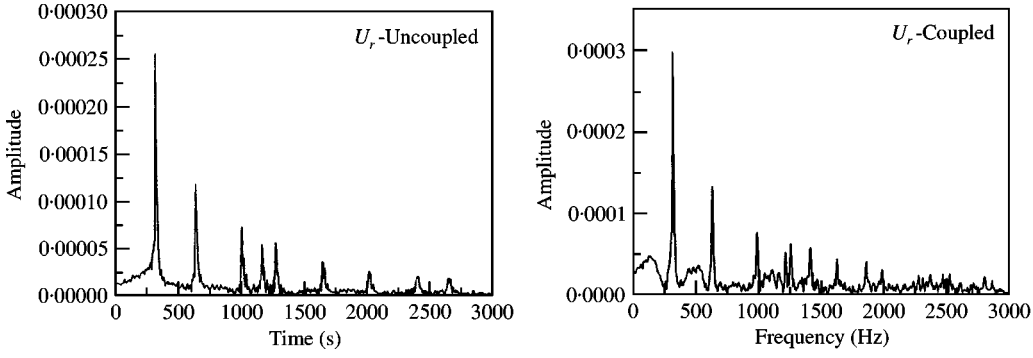

Figure 2. Uncoupled and coupled frequency response of displacement u_r to a centered impact.

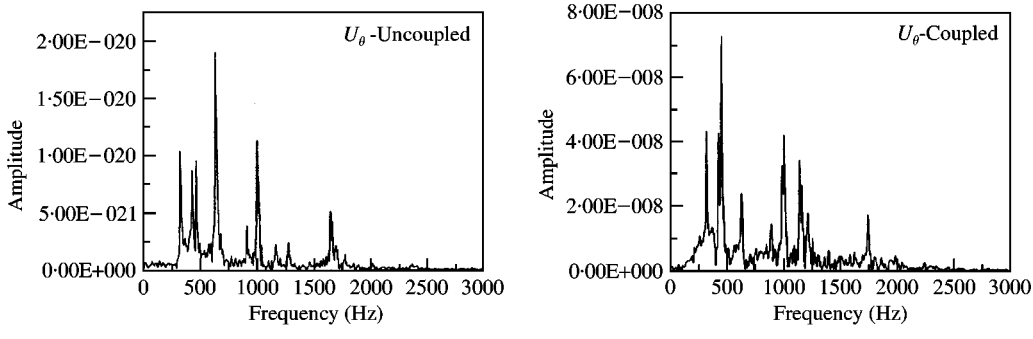

Figure 3. Uncoupled and coupled frequency response of displacement u_θ to a centered impact.

7.1. SYSTEM DYNAMICS

The cylindrical panel is excited by an impulse $q_r = \delta(x-(a_1+a_2)/2)\,\delta(\theta-(\alpha_1+\alpha_2)/2)\,\delta(t)$, $q_x = q_\theta = 0$ at its center. The natural frequencies of the cylindrical panel are listed in Table 2. For brevity, not all the resonant frequencies of the interior acoustic field are included here, but the first four ones are 354·0, 405·6, 479·5 and 566·9 Hz respectively. The responses of the fully coupled system and the system without the structural acoustic

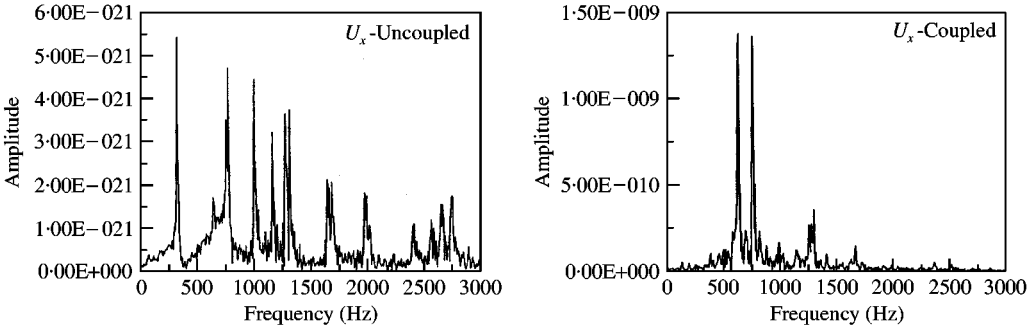

Figure 4. Uncoupled and coupled frequency response of displacement u_x to a centered impact.

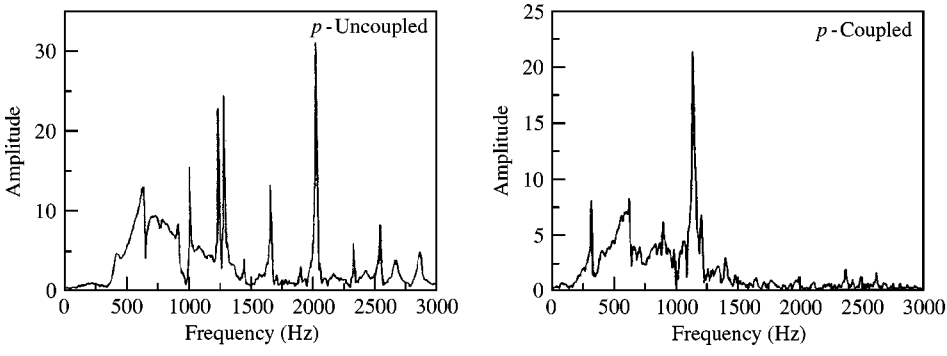

Figure 5. Uncoupled and coupled frequency response of acoustic pressure to a centered impact.

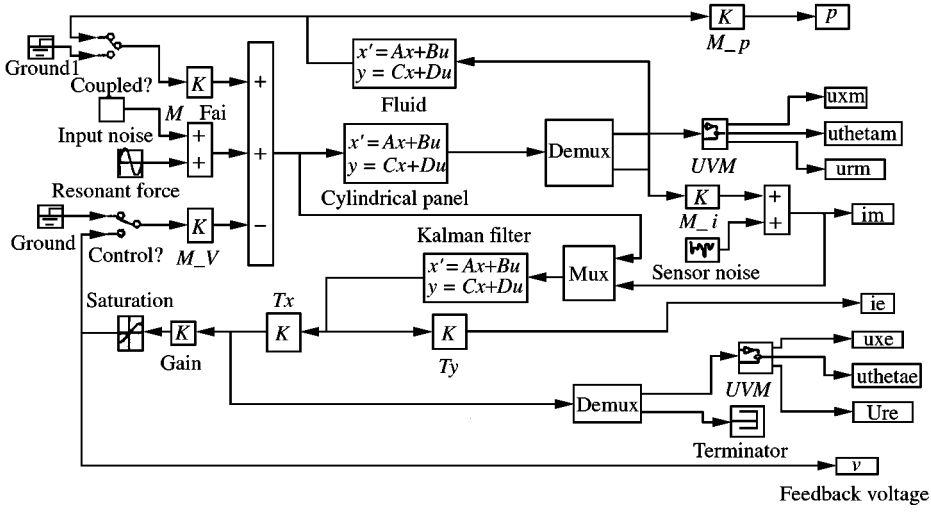

Figure 6. The MATLAB/Simulink mode for LQG vibration and noise control.

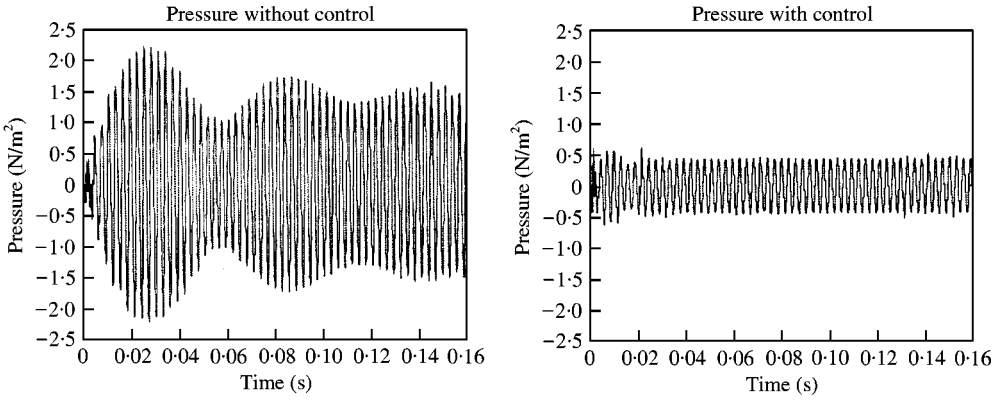

Figure 7. Acoustic pressure at the point $(r, \theta, x) = (R/2, L/2, 0)$ without/with control.

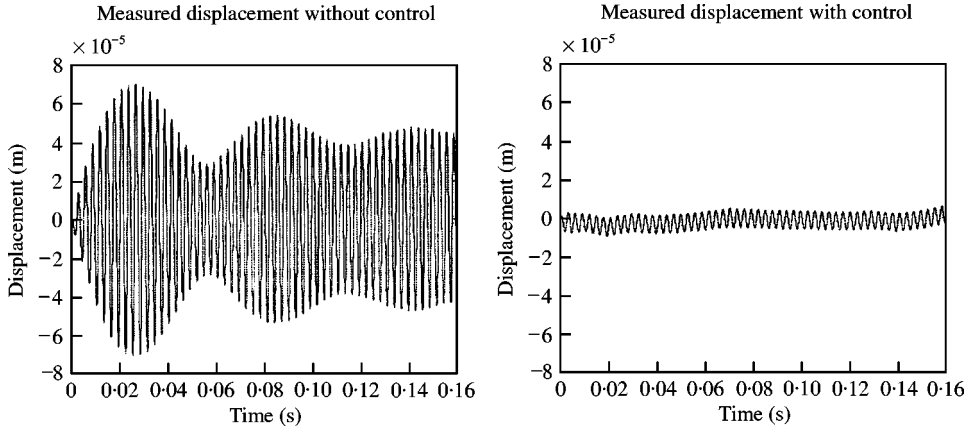

Figure 8. Measured displacement u_r at the center of the cylindrical panel without/with control.

coupling are simulated in this case. Note that in the system without structural acoustic coupling, the response of the panel can be transferred into the acoustic pressure, but the interior acoustic loading on the panel is neglected. The uncoupled and coupled frequency responses of the displacements u_r, u_θ and u_x are plotted in Figures 2, 3 and 4 respectively. It can be seen that the fully coupled system responses are at slightly lower frequencies than the one without the structural acoustic coupling. For example, the responses of displacement u_r at 322·09 Hz is slightly lower than the uncoupled natural frequency 325.69 Hz. The uncoupled and coupled frequency response of the cavity is plotted in Figure 5. It indicates that some resonant peaks of the acoustic pressure oscillation in the fully coupled system are enhanced due to the oscillation of the cylindrical panel while some resonant peaks of the acoustic pressure oscillation are decreased by the oscillation of the cylindrical panel. The same situations remain in the oscillation of the cylindrical panel.

7.2. RESONANT EXCITATION

As both the cylindrical panel and the acoustic field are resonant in the frequency range from 325·3 to 354·0 Hz, the exciting force is chosen as $q_x = q_\theta = 0$,

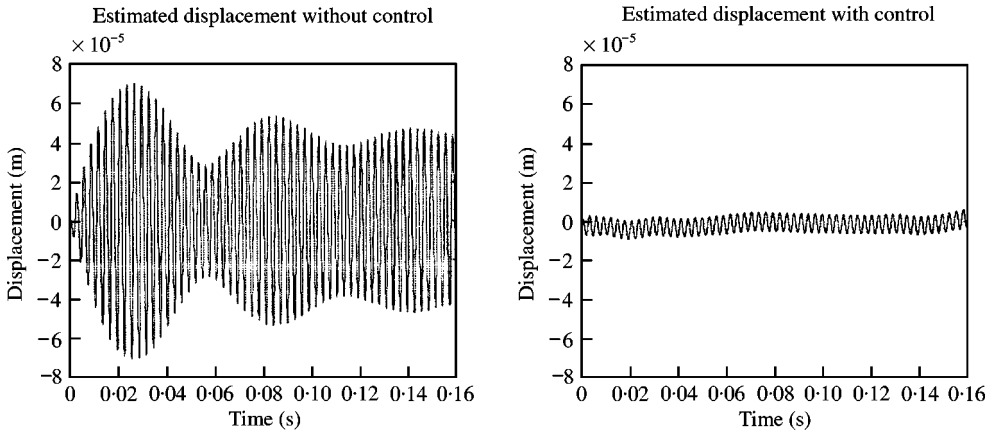

Figure 9. Estimated displacement u_r at the center of the cylindrical panel without/with control.

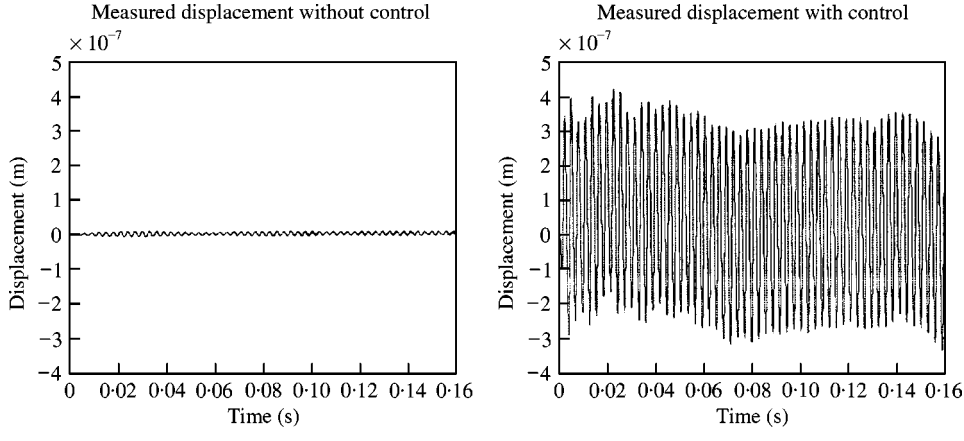

Figure 10. Measured displacement u_θ at the center of the cylindrical panel without/with control.

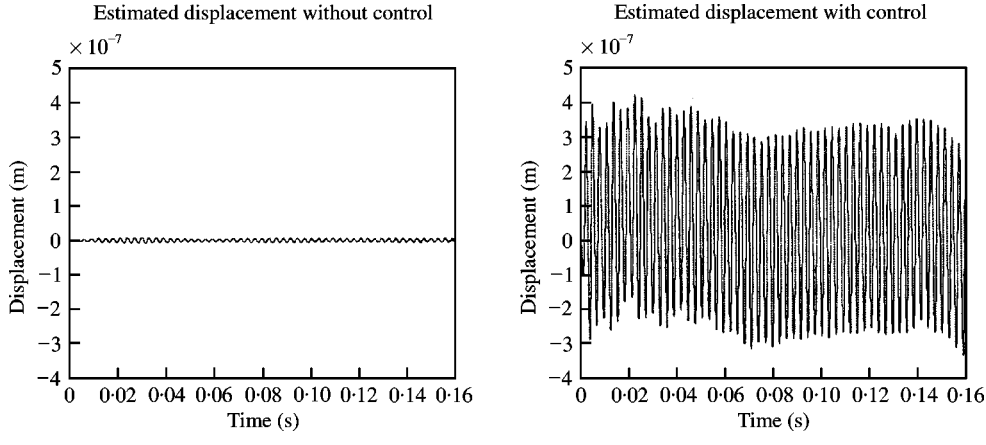

Figure 11. Estimated displacement u_θ at the center of the cylindrical panel without/with control.

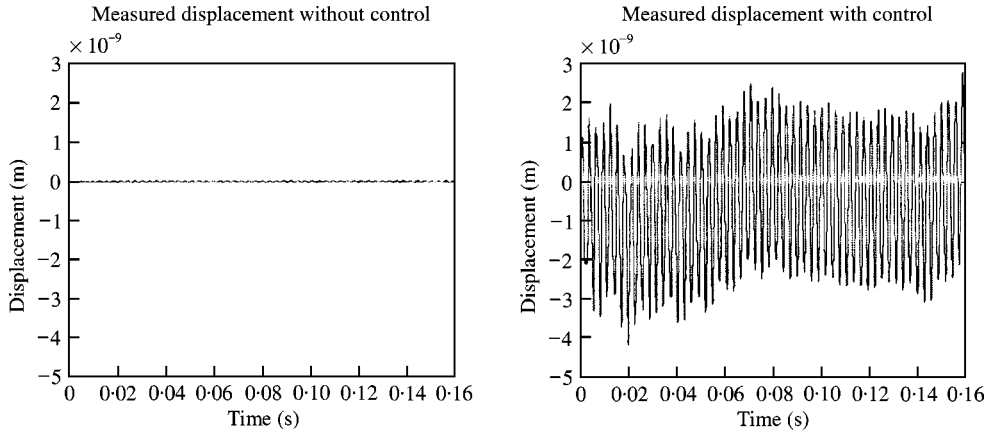

Figure 12. Measured displacement u_x at the center of the cylindrical panel without/with control.

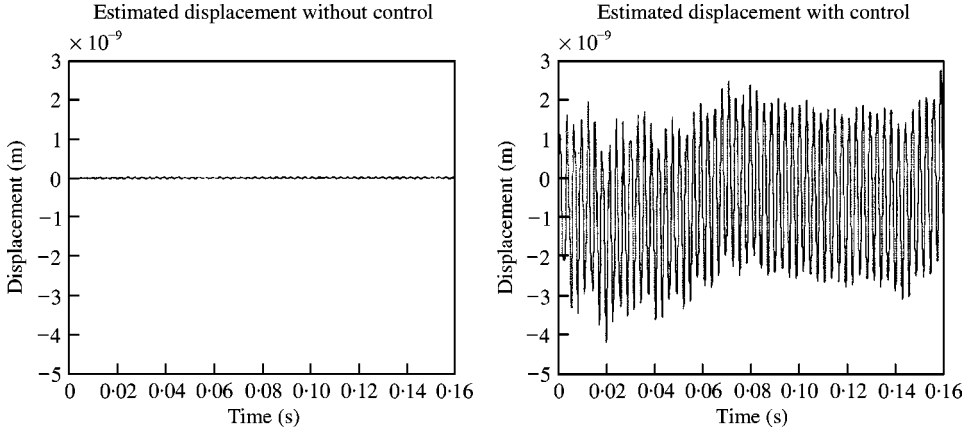

Figure 13. Estimated displacement u_x at the center of the cylindrical panel without/with control.

$q_r = 100 \sin(2{\cdot}1\pi \times 325{\cdot}3t)$. In addition, the process noise covariance is $\hat{Q} = 0{\cdot}001 Q_f$ and the measurement noise covariance $\hat{R} = 0{\cdot}001$. Control was implemented via a piezoelectric actuator bonded on the cylindrical panel and the optimal control voltage is determined by the optimal gain and all the states of the cylindrical panel which can be estimated from the output of the piezoelectric sensor using the Kalman filter. The simulation results are obtained from the model developed in section 5 and the MATLAB/Simulink model as shown in Figure 6. The acoustic pressure at the center of the cavity without/with control is plotted in Figure 7. Figures 8 and 9 show the responses of the measured and estimated displacement u_x at the center of the cylindrical panel without/with control respectively. It can be seen from Figures 7–9 that the acoustic pressure and the vibration of the cylindrical panel can be reduced considerably by applying the optimal control voltage on the piezoelectric actuator. The responses of the measured and estimated displacement u_θ at the center of the cylindrical panel without/with control are plotted in Figures 10 and 11. Figures 12 and 13 show the measured and estimated displacement u_x at the center of the cylindrical panel without/with control. Figures 10–13 indicate that the responses of the displacement u_θ and u_x is enhanced by the optimal control voltage. The measured and

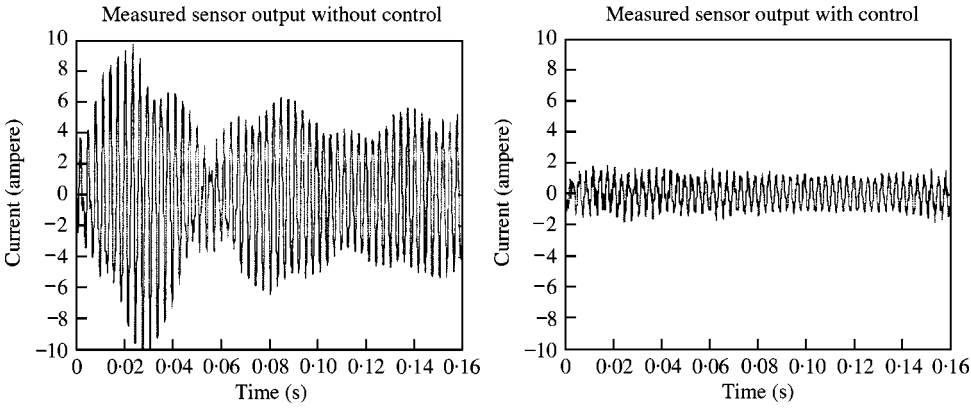

Figure 14. Measured output current of sensor without/with control.

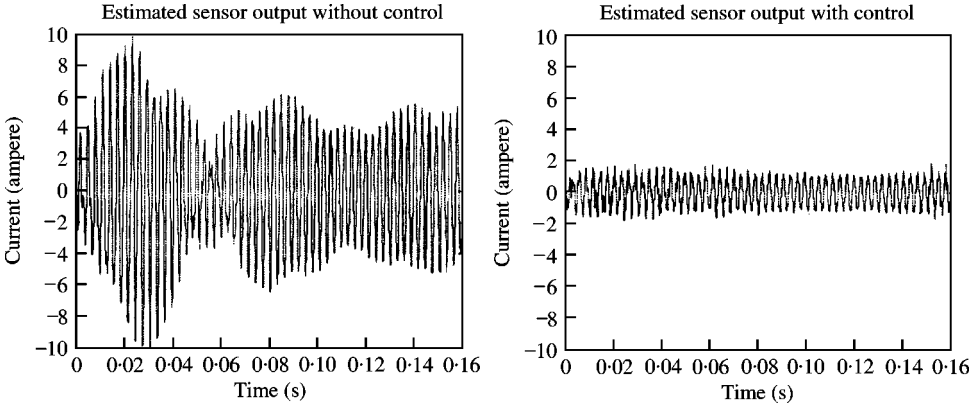

Figure 15. Estimated output current of sensor without/with control.

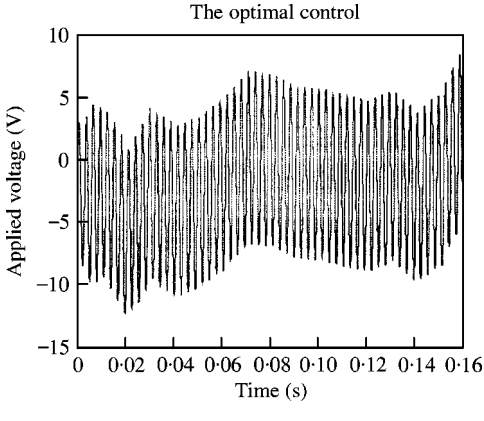

Figure 16. Optimal control voltage.

estimated output currents of the piezoelectric sensor without/with control are shown in Figures 14 and 15. It can be seen from Figures 8–15 that all the states can be estimated through the Kalman filter from the signal measured by the piezoelectric sensor. This is because the system as described by the state-space equation (27) is observable and stable; moreover, the measurement noise is much less than the sensor output. The optimal control voltage is shown in Figure 16. It should be noted that the magnitude of controlling voltage remains less than 10 V which is a physically reasonable voltage to put into the piezoelectric actuator. In order to keep the piezoelectric patch working in its safe voltage range, the performance weighting and the control effort penalty should be set reasonably. In order to maintain the system as controllable and observable and to reduce the structural borne noise more effectively and achieve high performance of the system, the number, sizes, locations of the piezoelectric actuators and sensors should be optimized in designing piezoelectric active structures for noise control [13–18].

8. CONCLUSION

This paper continued the active vibration and noise reduction of the structural acoustic coupled system. The numerical simulations are illustrated. The results demonstrate that such an LQG control system can significantly reduce the structural borne noise.

REFERENCES

1. V. JAYACHANDRAN and J. Q. SUN 1998 *Smart Materials and Structures* **7**, 72–84. Modeling shallow-spherical-shell piezoceramic actuators as acoustic boundary control elements.
2. J. D. JONES and C. R. FULLER 1987 *Proceedings of the Noisecon*, Pennsylvania, USA. 413–418. Active control of sound fields in elastic cylinders by vibrational inputs.
3. C. R. FULLER, R. J. SILCOX, V. L. METCALF and D. E. BROWN 1989 *Proceedings of the IEEE American Control Conference*, Pittsburgh, USA. Experiments on the structural control of sound transmitted through an elastic plate.
4. C. R. FULLER 1990 *Journal of Sound and Vibration* **136**, 1–15. Active control of sound transmission/radiation from elastic plates by vibration inputs: I. Analysis.
5. C. R. FULLER 1992 *Journal of Sound and Vibration* **153**, 387–402. Active control of sound transmission/radiation from elastic plates by vibration inputs: II. Experiments.
6. R. L. CLARK and C. R. FULLER 1991 *Journal of Intelligent Material Systems and Structures* **3**, 431–452. Control of sound radiation with adaptive structures.
7. E. K. DIMITRIADIS and C. R. FULLER 1991 *American Institute of Aeronautics and Astronautics Journal* **29**, 1771–1777. Active control of sound transmission through elastic plates using piezoelectric actuators.
8. S. J. ELLIOTT, P. A. NELSON, I. M. STOTHERS and C. C. BOUCHER 1990 *Journal of Sound and Vibration* **140**, 219–238. In-flight experiments on the active control of sound and vibration.
9. J. Q. SUN, M. A. NORRIS, D. J. ROSSETTI and J. H. HIGHFILL 1996 *Journal of Vibration and Acoustics* **118**, 676–681. Distributed piezoelectric actuators for shell interior noise control.
10. F. FAHY 1985 *Sound and Structural Vibration*. London: Academic Press.
11. W. FLÜGGE 1973 *Stresses in Shells*. Berlin: Springer-Verlag; New York: Heidelberg.
12. J. H. HAN, K. H. REW and I. LEE 1997 *Smart Materials and Structures* **6**, 549–558. Experimental study of active vibration control of composite structures with a piezoelectric-ceramic actuator and a piezo-film sensor.
13. R. L. CLARK and C. R. FULLER 1992 *Journal of Acoustical Society of America* **91**, 3313–3320. Experiments on active control of structurally radiated sound using multiple piezoceramic actuators.
14. R. L. CLARK and C. R. FULLER 1992 *Journal of Acoustical Society of America* **92**, 1521–1533. Optimal placement of piezoelectric actuators and polyvinylidene fluoride error sensors in active structural acoustic control approaches.

15. B. T. WANG, R. A. BURDISSO and C. R. FULLER 1994 *Journal of Intelligent Material Systems and Structures* **5**, 67–77. Optimal placement of piezoelectric actuators for active structural acoustic control.
16. B. T. WANG 1996 *Journal of Acoustical Society of America* **99**, 2975–2984. Optimal placement of microphones and piezoelectric transducer actuators for far-field sound radiation control.
17. J. KIM and B. KO 1998 *Smart Materials and Structures* **7**, 801–808. Optimal design of a piezoelectric smart structure for noise control.
18. J. H. KIM, S. B. CHOI, C. C. CHEONG, S. S. HAN and J. K. LEE 1999 *Smart Materials and Structures* **8**, 1–12. H_∞ control of structure-borne noise of a plate featuring piezoelectric actuators.